TOPICAL REVIEW

Pressure induced topological and topological crystalline insulators

IOP Publishing Journal of Physics: Condensed Matter
J. Phys.: Condens. Matter **34** (2022) 423001 (16pp) https://doi.org/10.1088/1361-648X/ac8906

Topical Review

Pressure induced topological and topological crystalline insulators

V Rajaji[1,2,3,*], F J Manjón[4] and Chandrabhas Narayana[2,3,*]

[1] University Lyon, Université Claude Bernard Lyon 1, CNRS, Institut Lumière Matière, F-69622 Villeurbanne, France
[2] Chemistry and Physics of Materials Unit, Jawaharlal Nehru Centre for Advanced Scientific Research, Jakkur PO, Bangalore 560 064, India
[3] School of Advance Materials, Jawaharlal Nehru Centre for Advanced Scientific Research, Jakkur PO, Bangalore 560 064, India
[4] Instituto de Diseño para la Fabricación y Producción Automatizada, MALTA Consolider Team, Universitat Politècnica de València, 46022 Valencia, Spain

E-mail: rajaji.vincent@univ-lyon1.fr and cbhas@jncasr.ac.in

Received 4 April 2022, revised 26 July 2022
Accepted for publication 11 August 2022
Published 23 August 2022

Abstract

Research on topological and topological crystalline insulators (TCIs) is one of the most intense and exciting topics due to its fascinating fundamental science and potential technological applications. Pressure (strain) is one potential pathway to induce the non-trivial topological phases in some topologically trivial (normal) insulating or semiconducting materials. In the last ten years, there have been substantial theoretical and experimental efforts from condensed-matter scientists to characterize and understand pressure-induced topological quantum phase transitions (TQPTs). In particular, a promising enhancement of the thermoelectric performance through pressure-induced TQPT has been recently realized; thus evidencing the importance of this subject in society. Since the pressure effect can be mimicked by chemical doping or substitution in many cases, these results have opened a new route to develop more efficient materials for harvesting green energy at ambient conditions. Therefore, a detailed understanding of the mechanism of pressure-induced TQPTs in various classes of materials with spin–orbit interaction is crucial to improve their properties for technological implementations. Hence, this review focuses on the emerging area of pressure-induced TQPTs to provide a comprehensive understanding of this subject from both theoretical and experimental points of view. In particular, it covers the Raman signatures of detecting the topological transitions (under pressure), some of the important pressure-induced topological and TCIs of the various classes of spin–orbit coupling materials, and provide future research directions in this interesting field.

Keywords: topological insulators, high pressure, strong spin–orbit coupling, topological crystalline insulators, optical spectroscopy, phonons, quantum materials

(Some figures may appear in colour only in the online journal)

* Authors to whom any correspondence should be addressed.

1. Introduction

In addition to the well-known electronic states of matter such as an insulator, semiconductor, and metal, recent theoretical and experimental discoveries have established topological insulators (TIs) [1–3]. TIs are a new class of quantum matter in which bulk is insulating, but the surface is conducting via helical spin states [1]. Therefore, in a highly simplified picture, the newly discovered TIs can be viewed as insulating plastic material covered with metallic wires. The conducting surface states intrinsically originate due to strong spin–orbit coupling (SOC) and are protected by time-reversal symmetry. Due to this special protection, surface states are very robust against chemical disorders and non-magnetic impurities. Therefore, TIs are not only attractive for their fundamental scientific importance, but also their potential application possibilities in quantum computation, spintronics, and thermoelectrics [1].

At first, HgTe/CdTe quantum well was predicted to be a promising material for the 2D TI at ambient conditions [2], and then the existence of helical edge states were confirmed by charge-transport experiments [3]. Soon after this great discovery, various 3D TIs were predicted in strong SOC compounds [4]. One of the important 3D TIs belongs to the tetradymite-type A_2X_3 (A = Bi, Sb and X = Se, Te) family. The compounds belonging to this family, such as Bi_2Te_3, Bi_2Se_3, and Sb_2Te_3 show surface states (single Dirac-like cone) at Γ point of the Brillouin zone (BZ) at ambient conditions and were confirmed by a surface-sensitive technique like angle resolved photo emission spectroscopy (ARPES) [5–7].

The topological invariant quantity $\mathbb{Z}_2$ is the order parameter that is used to characterize and classify the TIs. For instance, there are four $\mathbb{Z}_2$ topological invariants (ν_0; ν_1, ν_2, ν_3) utilized for classifying the 3D Tis [8]. When $\nu_0 \neq 0$, the system is a strong 3D TI. If $\nu_0 = 0$, then the system will be classified based on the values of (ν_1, ν_2, and ν_3). Furthermore, when $\nu_1 = 0$, $\nu_2 = 0$, and $\nu_3 = 0$, the system is a conventional or normal insulator (NI). But when any of these three quantities are not zero; then, the system will be called a weak TI. For instance, Bi_2Se_3 is a strong TI [(1; 000) and $\mathbb{Z}_2 = 1$] and BiSe is a weak TI (0; 001) [9]. Mathematically, $\mathbb{Z}_2$ is the product of parities of the bands at time-reversal invariant momenta (TRIM) points in the BZ [1, 8] and the Z2PACK code (a more robust and accurate method) is available to calculate it theoretically [10].

Topological crystalline insulators (TCIs) are another interesting class of non-trivial topological materials in which the surface states are protected by a crystal mirror symmetry [11, 12]. Therefore, TCI's surface states are robust against magnetic dopants or impurities, whereas that of TIs are not. Further, in sharp contrast to TIs that has an odd number of band inversions (BIs), TCIs has an even number of BIs. Mirror Chern number n_M is used to characterize the TCI phase in general, which can be written as $n_M = (C_{+i} - C_{-i})/2$ [1, 11, 12]. Here C_{+i} and C_{-i} denote the individual Chern numbers associated with a mirror-invariant plane. For instance, the Pb rich pseudo binary systems such as $Pb_{0.6}Sn_{0.4}Te$ and $Pb_{0.77}Sn_{0.23}Se$, have been experimentally shown to be TCI [13, 14].

Some NIs can be converted into TIs by tuning the SOC strength of the compounds [15]. The process of transformation from NI to TI is called a 'topological quantum phase transition' (TQPT) [16]. In general, tuning of SOC strength can be achieved by chemical doping or substitution [15] since SOC strength is mainly determined by chemical composition (it increases for heavier elements as it goes with Z^4, being Z the atomic number). However, external parameters, like pressure or strain [17–20], temperature [21–23], electric field [17], etc can help in inducing the TQPT in NIs whose SOC are not strong enough to be TIs at ambient conditions. Among these external parameters, pressure is one of the ideal routes for this transformation because of its effective and cleaner nature.

How can pressure help in inducing a TQPT? Pressure is a thermodynamic parameter that allows a finely tuning of the volume, lattice parameters, bond lengths, effective hybridization, electron density, and crystal field splitting of materials [18, 19, 24–26]. These parameters affect the electronic band structure of the material that could lead to a decrease in the band gap and help the SOC to produce a BI [18–20, 25, 27]. Therefore, some 3D NIs with a relatively weak SOC can be converted into 3D TIs by increasing pressure [16, 18, 24, 28].

The schematic process of a pressure-induced TQPT is shown in figure 1. The driving force for the pressure-induced TQPT is the decrease, closing, and subsequent reopening of the band gap that occurs with the increase of pressure in some materials with a relatively weak SOC in which the band gap at room pressure is too large to induce a BI. The decrease of the band gap with increasing pressure allows these NIs with SOC to turn into a TI or a TCI through an intermediate state (3D topological Dirac semimetal) at P_c in which the band gap is fully closed and a Dirac cone is formed (see figure 1). Note that, some strong SOC materials with narrow band gaps lead to a BI and therefore the material is already a TI or a TCI at room pressure (examples: Bi_2Se_3, Sb_2Te_3, and Bi_2Te_3) [5–7]. Paradigmatic examples of pressure-induced TQPTs are those theoretically proposed for the rhombohedral phase of As_2Te_3 (β-As_2Te_3) [29, 30] and β-Sb_2Se_3 [19, 27]. These compounds are NIs at ambient conditions due to their wider band gap and the relatively weak SOC strength. But, in these compounds, pressure can help in inducing the BI by decreasing the band gap as already commented.

The pressure-induced topological transitions have been shown to greatly influence the thermoelectric performance of some compounds [31, 32]. The BI leads to an increase in the density of states (DOS) near the Fermi level, electrical conductivity, Seebeck coefficient, and therefore enhancement in the thermoelectric performance of the material [32]. For example, recent high-pressure experiments on Cr doped PbSe (i.e. $Pb_{0.99}Cr_{0.01}Se$) showed a higher thermoelectric figure of merit (ZT) value during the TCI transition [31]. At ambient conditions, $Pb_{0.99}Cr_{0.01}Se$ compound show ZT of about

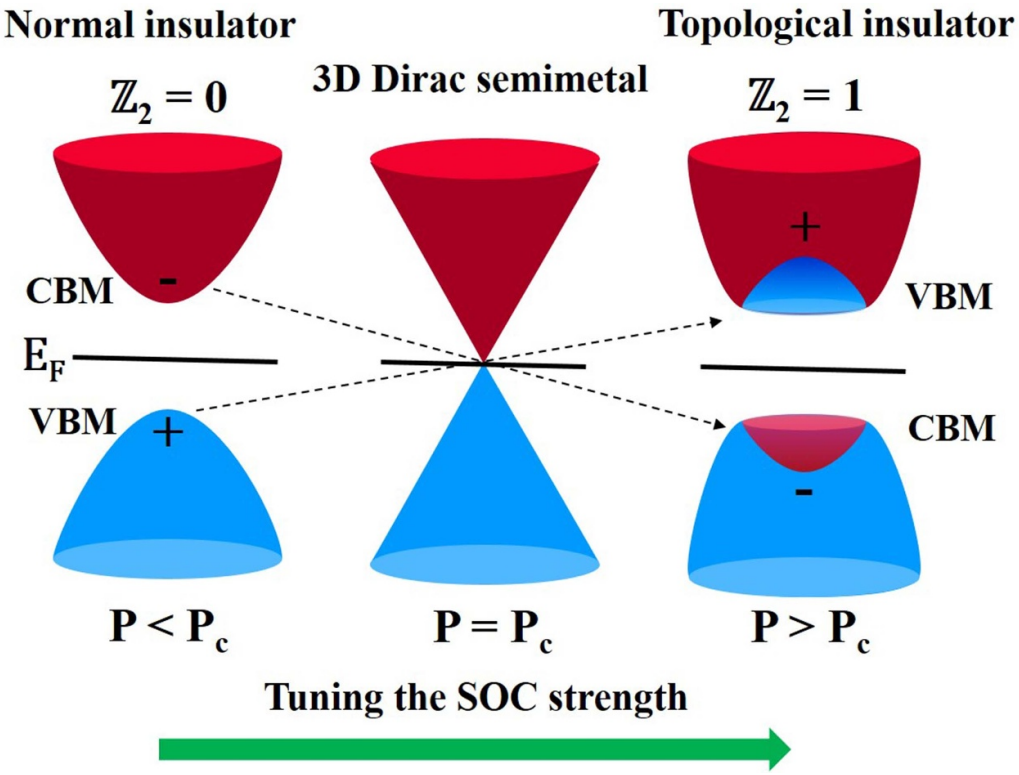

Figure 1. Schematic of the typical band inversion (BI) associated with the pressure-induced TQPT. The pressure-induced TQPT occurs due to the decrease, closing, and subsequent reopening of the band gap that occurs as pressure increases. This process usually occurs on increasing the SOC strength (for instance by chemical doping or substitution). Here, P_c represents the critical transition pressure at which the TQPT occurs because of the closing of the band gap. The $-$ and $+$ signs indicate the odd and even parity of the bands at the TRIM point, respectively. The BI is evidenced by the change in the parity of the valence band maximum (VBM) and conduction band minimum (CBM) that occurs above P_c.

$\sim$0.45. Under pressure, the ZT is enhanced up to $\sim$1.7 (at a pressure of 2.8 GPa and at room temperature) [31]. This remarkable enhancement originates from the TCI transition at $\sim$2.8 GPa in L point of the BZ [31]. This experiment strongly established the relationship between topological transitions and thermoelectric enhancement. Therefore, the discovery and understanding of the topological materials will be very useful to improve the technological aspects of thermoelectrics and effectively contribute to the development of green energy generators.

In this review, we mainly focus on the pressure-induced TQPTs studied in different families of materials with SOC and the detection of the Raman signatures of topological transitions at high pressures and its interpretation with the help of *ab initio* calculations. We first briefly discuss the common criteria for identifying pressure-induced TIs and TCIs from a theoretical and experimental perspective. Further, we will discuss the effect of pressure on the electronic band structure of topological materials and emphasize the importance of the Raman signatures in pressure-induced TQPTs. We summarize some of the essential pressure-induced TIs and TCIs explored so far, the interconnection between them, the open questions, and finally suggest the possible future directions of this interesting research field.

2. Search for the pressure-induced topological materials (TIs and TCIs)

The following important criteria [1, 8] should be satisfied to classify a material as a TI or a TCI: (a) The VBM and CBM should cross and form a BI at TRIM points of the BZ. (ii) The parity associated with the bands of VBM and CBM should exchange each other during the BI. (iii) The topological invariant quantities ($\mathbb{Z}_2$ for TI and n_M for TCI) should change during the TQPT. Nowadays, there is a straightforward procedure available (from Z2PACK code) [10] to calculate the topological invariant quantities, and using this, many materials are potentially identified as pressure-induced TIs and TCIs. Therefore, first-principles theoretical calculations play a crucial role in predicting the pressure-induced TQPTs.

First-principles calculations are in many cases easier and faster than experimental techniques to determine and classify topological materials and predict TQPTs; however, there are also some roadblocks in theoretical calculations. On one hand, standard calculations based on the density functional theory (DFT) use to underestimate the band gap so they can make a wrong classification of topological materials unless more complex calculations are performed. On the other hand, some predictions reported in the literature for several materials are

unrealistic because those compounds have not been synthesized to date; i.e. the calculations were done for a hypothetical crystal structure that does not correspond to the crystal structure known at ambient conditions. One example of this last case corresponds to theoretical calculations of the rhombohedral phase (tetradymite-like) of the Sb_2Se_3 (β-Sb_2Se_3). This compound has been predicted either to be a TI at room pressure [33], or to be a TI under strain and hydrostatic pressure [19, 27]. Unfortunately, Sb_2Se_3 always crystallizes in the orthorhombic structure at ambient conditions [34, 35]. Only recently, its existence in a few-layers thin film has been shown and its structural stability at room temperature conditions fully discussed [36, 37]. Therefore, the existence of a pressure-induced TQPT in β-Sb_2Se_3 is far from being experimentally demonstrated. This example shows that the predicted TI properties of some materials might not occur in real life. One more critical point to be added to the reported theoretical prediction is the nature of the strain applied. In theoretical approaches, it is possible to implement all kinds of strains such as uniaxial, biaxial, and hydrostatic (both compression and tension). However, it is essential to note that hydrostatic (isotropic) pressure (compression) is the most common, controlled, and experimentally easily accessible strain using a diamond anvil cell (DAC), which easily generates pressures in the order of GPa. Hence, hydrostatic pressure-dependent calculations are more important for practical aspects. In summary, the crystal structure, band gap, and the kind of strain reported in the theoretical predictions should be of concern for an experimentalist before they embark on the experiments on the predicted topological transitions in materials.

3. Pressure effect on the electronic structure of topological materials

As BI is one of the fundamental criteria for TQPT, the detailed discussion of pressure evolution of the electronic band structure will be crucial and discussed in the literature for all the pressure-induced topological materials [18–20, 38]. Therefore, to illustrate the idea of the effect of high pressure on the band structure of the topological materials, here we have briefly discussed one of the promising pressure-induced TI, β-As_2Te_3 [29]. The process of the pressure-induced TQPT in β-As_2Te_3 is represented in figures 2(a)–(c) [29]. At 0 GPa, the calculated electronic structure of β-As_2Te_3 using the quasiparticle self-consistent GW methodology and the inclusion of the SOC reveals an indirect band gap of 0.30 eV (see figure 2(a)). As pressures increases to 2 GPa, the band gap closes and the compound becomes a 3D topological Dirac semimetal with Dirac cones at the Γ point (see figure 2(b)) [29]. At higher pressures the band gap reopens and the compound becomes a TI (see figure 2(c)). As expected, the calculated $\mathbb{Z}_2$ topological invariant numbers for the β-As_2Te_3 compound at 0 GPa and 4.0 GPa give the values of (0; 000) and (1; 000) [29]. In this context, it must be mentioned that many works in the literature represent the pressure evolution of the band gap and isosurfaces of charge density for VBM and CBM

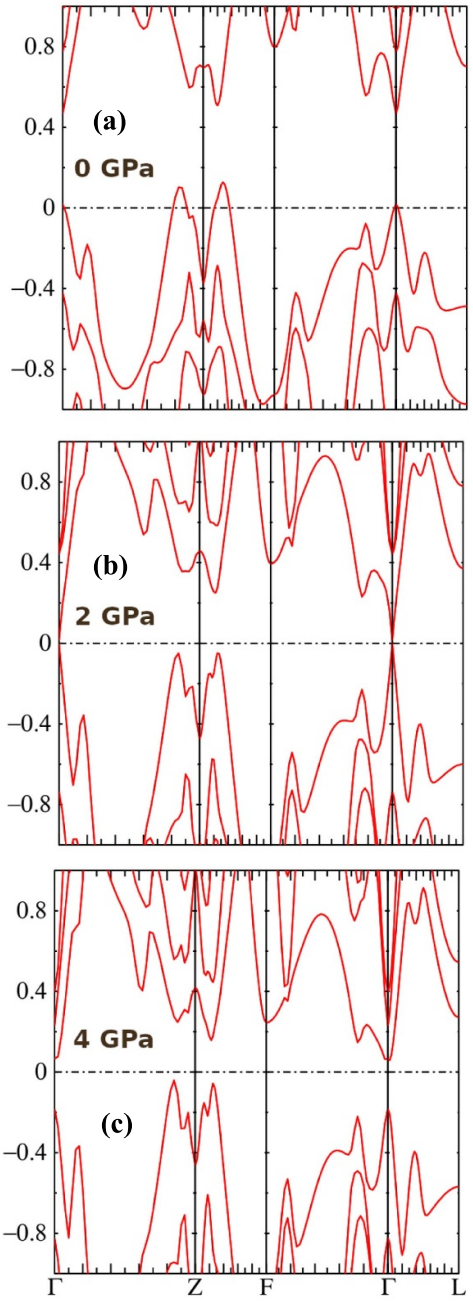

Figure 2. Theoretically calculated hydrostatic pressure dependent electronic band structure of β-As_2Te_3 at (a) 0 GPa (top), (b) 2.0 GPa (middle), and (c) 4.0 GPa (down). The BI signature (W shaped) is evidenced at the Γ point of the BZ near to Fermi level. This figure is adopted from [29].

[39, 40]. It might be mainly due to easier representation of BI and to visualize their features.

Regarding theoretical calculations of pressure-induced TQPTs, it is important to note that the accuracy in the prediction of the pressure at which a TQPT occurs in topological materials depends on the accuracy of the electronic band structure calculations; i.e. on how the calculations approach the absolute values of the band gap in real materials. Generally, the accuracy of the calculations depends on

the exchange-correlation potential and the effect of SOC of the compound. Since SOC is one of the key reasons for the TQPT, it is important to include the SOC effect in the topological property calculations [19, 27, 29, 30]. In this context, we must note that standard first-principles DFT calculations using the local density approximation or the generalized gradient approximation (GGA) tend to underestimate the band gap. However, some works suggest that there are exceptions, like GaGeTe, in which GGA + SOC calculations show better agreement with experiments than hybrid Heyd–Scuseria–Ernzerhof (HSE06) + SOC calculations [41]. Therefore, caution must be taken when predicting pressure-induced TQPTs because there can be a significant mismatch between the experimental and theoretical band gap that can alter considerably the pressure at which the TQPT occurs.

In addition to pressure-induced TQPTs, various interesting pressure-driven electronic transitions are observed in different classes of materials due to the pressure-induced changes in the electronic band structure [42–44]. In particular, for the case of some topological materials, Lifshitz transitions or electronic topological transitions (ETTs) are observed under high-pressure conditions [45, 46]. An ETT occurs when a band extremum, associated to a Van Hove singularity in the electronic density of states (EDOS), crosses the Fermi energy. This crossing leads to a strong redistribution of the EDOS near the Fermi energy that causes an isostructural phase transition of electronic origin; i.e. of order higher than 2 in the Ehrenfest classification. Therefore, there is no volume discontinuity and no change in Wyckoff positions, but a change in the elastic constants and consequently in the compressibility [47, 48]. Therefore, it must be mentioned that, even though TQPT and ETT are named as topological transitions, they are two completely different phenomena and have no connection between them. Further, it is interesting to note that some ambient 3D TIs (Bi_2Se_3, Sb_2Te_3, and Bi_2Te_3) under hydrostatic pressure induce the ETT at around 3–4 GPa regions [46, 49–51]. Hence, caution must be taken also when predicting a TQPT since the closing of the band gap can be also associated to the presence of ETTs at similar pressures.

4. Raman scattering as an important indirect probe of pressure-induced TQPTs

The important question is how to detect the signature of topological transition under high-pressure conditions experimentally? The topological surface states at ambient conditions can be directly detected by several techniques, such as ARPES [5–7, 13, 14] and scanning tunneling microscopy (STM) [52]. But, one of the fundamental challenges is to characterize the formation of topological surface states under high-pressure conditions (in the order of GPa). Because, at present, the coupling of the DAC with ARPES or STM is beyond the potential technical limit. However, when there are sharp changes in the topology of the electronic band structure, it can be detected from bulk properties through some specific experiments. For example, we can use the Raman scattering technique to get the indirect signatures of topological transitions [40, 53–55]. During the TQPT process (see figure 1), we expect charge density fluctuations and changes in the electron–phonon coupling in the materials.

Recently, the theoretical model Hamiltonian calculations gave a detailed picture of the relationship between the topological transition (BI) and Raman linewidth [56]. Mathematically, it is shown that the Raman line width is directly proportional to the square of the energy-resolved electron-phonon matrix elements [56]. Hence, the dynamics of electron–phonon coupling strongly captures the topological transitions through full width at half maximum (FWHM) of a Raman mode. In particular, for the case of a centrosymmetric crystal, zone center optical phonons (long wavelength, i.e. $q \sim 0$) can potentially couple to electrons through commutation or anti-commutation with an electronic parity operator [56]. Hence, the Raman linewidth indirectly measures the BI and acts as a good indicator of topological invariant changes in the system. In this way Raman scattering is an effective tool to investigate the electron–phonon coupling changes [40, 53]. Using this principle, Raman linewidth anomalies evidenced the topological transitions in various SOC systems like BiTeI, 1T-$TiTe_2$, 1T-$TiSe_2$, Sb_2Se_3, $TlBiS_2$, etc, and the details will be discussed in the below sections [39, 40, 53–55]. Similar to Raman scattering, signatures of the BI; i.e. band gap closing and reopening can also be obtained by infrared (IR) spectroscopy measurements at high-pressure [24]. It must also be noted that electron–phonon coupling changes and charge density redistributions can also be detected by electrical transport measurements [53, 57]. Therefore, several experimental techniques can be used to indirectly detect changes in the topology of the electronic band structure at high pressure conditions. We want to highlight here that Raman spectroscopy is the easiest experimental technique that can be used to get an insight about the pressure-induced TQPTs in SOC materials.

Note that the Raman scattering is a qualitative microscopic tool, and any changes (or transitions) such as magnetic and electronic transitions, metallization, Lifshitz transitions, and structural phase transitions will be reflected in its frequency, lifetime (inversely proportional to line width) and intensity. Therefore, to confirm that it is indeed an electronic transition (say topological transitions), we need to use multiple experimental tools that will carefully rule out the possibility of any other transitions, and the results should be confirmed with the first-principles theoretical calculations. In summary, the coupling of multiple experiments such as Raman scattering, synchrotron XRD and electrical transport along with the first-principles calculations is an efficient way to study the pressure-induced TQPTs [53].

5. Pressure-induced TQPTs in different classes of materials

5.1. A_2X_3 compounds

The study of pressure-induced TQPTs in binary A_2X_3 compounds has been mainly carried out in tetradymite-type group-15 chalcogenides. The family of A_2X_3 (A = As, Sb, Bi; X = S, Se, Te) chalcogenides can be classified into

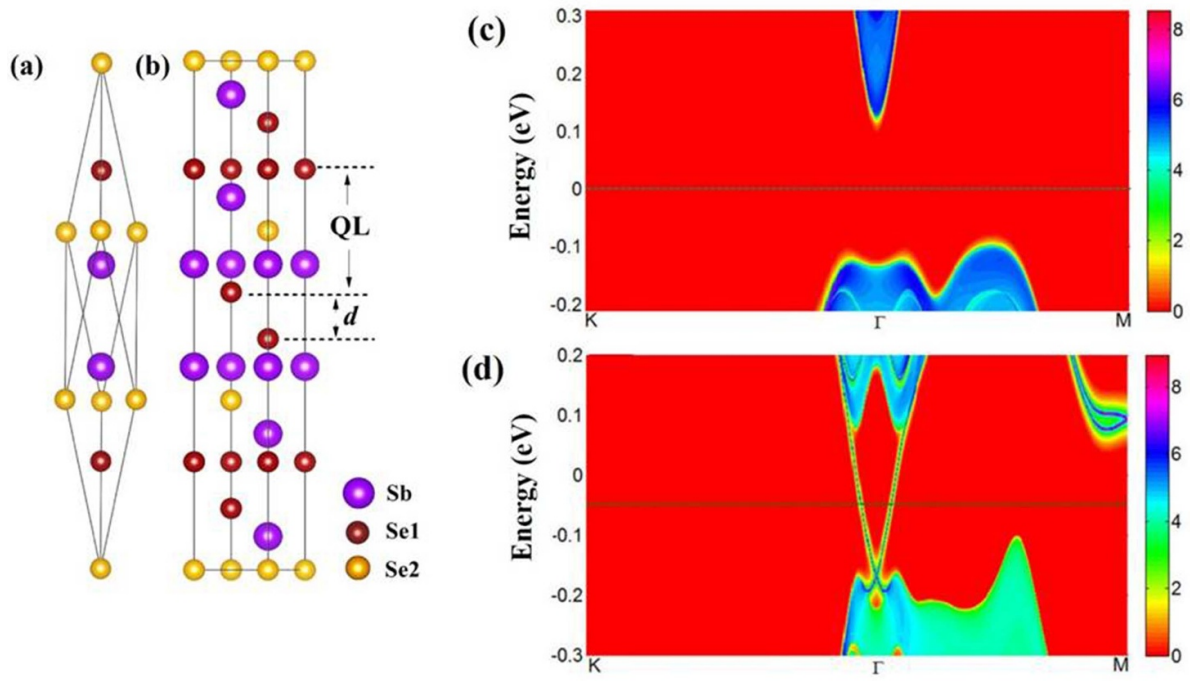

Figure 3. (a) Crystal structure of the rhombohedral phase of Sb_2Se_3 and (b) unit cell of Sb_2Se_3 in the hexagonal setting. Here QL and *d* represent the quintuple layers and interlayer distance, respectively. This figure is adopted from [33]. (c) Evolution of band structure of the surface spectral function for Sb_2Se_3 at ambient and (d) 3.0 GPa along the [111] surface. The green and red regions represent the bulk energy bands and bulk energy gaps, respectively. The dashed line signifies the Fermi level. The typical TQPT and Dirac-like topological surface states can be seen at Γ point of the BZ under the hydrostatic pressure 3.0 GPa. This figure is adopted from [19].

three classes based on the structure type. Heavier atoms lead to compounds with tetradymite (Bi_2Te_2S) structure, such as Bi_2Te_3 ($E_g \sim 0.12$ eV), Bi_2Se_3 ($E_g \sim 0.30$ eV), and Sb_2Te_3 ($E_g \sim 0.28$ eV). These chalcogenides show a layered rhombohedral crystal structure [space group (SG): $R\bar{3}m$, $Z = 3$] at ambient conditions [5, 45]. In these compounds, quintuple layers (X–A–X–A–X) are extended along the hexagonal *a–b* plane and these layers are piled up along the hexagonal *c* axis (see figure 3). Inside the layers, the bonds are a mixture of covalent and multicenter (also named metavalent or hypervalent) [58] types and between the layers, the bonds are van der Waals types [59, 60]. Therefore, these systems can be considered as 'quasi 2D' crystals. Due to the strong SOC and a narrow band gap, these systems are identified as second-generation 3D TIs, and all of them show a single Dirac cone at Γ point of the BZ [5–7]. In this class, it is important to include β-As_2Te_3 [29, 30] and β-Sb_2Se_3 [19, 27, 33, 36, 39] that are NIs due to insufficient SOC strength, as previously commented.

The second structural class from A_2X_3 family are Bi_2S_3 ($E_g \sim 1.30$ eV), Sb_2S_3 ($E_g \sim 1.7$–1.8 eV), and Sb_2Se_3 ($E_g \sim 1.00$ eV), which adopt the orthorhombic structure (SG: *Pnma*, $Z = 4$) at ambient conditions and are wide band gap semiconductors [61, 62]. As the structure of the material controls the properties, these systems are not TIs at either ambient or high-pressure conditions. Finally, the third class of this family is composed by As_2S_3, As_2Se_3, and α-As_2Te_3 that tend to crystalize in highly distorted monoclinic structures [42]. These compounds are also NIs at ambient conditions. To the best of our knowledge, no pressure-induced topological properties have been found to date on these compounds.

First-principles theoretical calculations predicted that the rhombohedral phase [hypothetical structure (see figure 3(a)) from the theoretical calculations aspect] of Sb_2Se_3 (β-Sb_2Se_3) undergoes into TI under external pressure [19, 27, 33]. Similar to other rhombohedral phase tetradymite compounds, Sb_2Se_3 shows the BI at Γ point of the BZ under pressure [19]. Interestingly, this system was demonstrated from theoretical calculation to exhibits TI properties under both uniaxial (along the *c* axis compression) and hydrostatic pressure, as shown in figure 3(d). In this context, Bera *et al* experimentally showed that the changes in the electron–phonon coupling through phonon (E_g mode) anomalies at ~2.5 GPa for the β-Sb_2Se_3 as represented in figure 4 [39]. This study claimed that linewidth anomalies of E_g mode is the signature of transition from NI to TI due to the changes in the topological invariant quantity ($\mathbb{Z}_2$) and complemented with the first-principles calculations based on the non-adiabatic treatment of phonons [39]. In fact, this is a pioneer experimental work for showing the topological transition using Raman scattering. However, this work was further questioned by several experimental research groups. We summarize the major ongoing debate of this claim below.

The first one is about the structure of the Sb_2Se_3 compound. Bera *et al* claimed the single-crystal synthesis of the $R\bar{3}m$ phase of Sb_2Se_3 [39]. But the synthesis of single-crystal was not supported (or proven) by any systematic structural

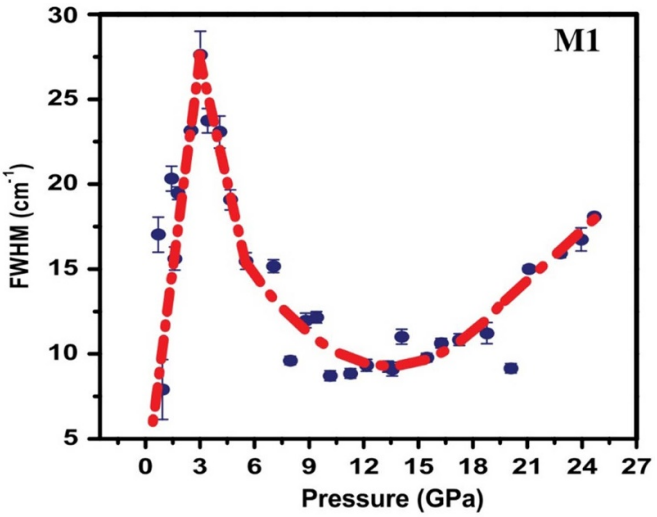

Figure 4. Pressure dependence of FWHM of M1 phonon mode (E_g) in the rhombohedral phase of Sb_2Se_3. The sharp maxima at ∼2.5 GPa signifies the TI transition. This figure is adopted from [39].

analysis such as single crystal XRD, microstructural characterization like TEM, etc. Mention must be made that the reported rhombohedral phase ($R\bar{3}m$ of Sb_2Se_3) observation in bulk form has not been verified to date by any other experimental group. Only a few-layer film of this phase seems to have been recently synthesized over a Bi_2Se_3 substrate [36]. Most of the experimental studies confirm that Sb_2Se_3 adopts an orthorhombic structure (SG: *Pnma*) at room temperature conditions [34, 35]. Hence the crystal structure of the single-crystalline Sb_2Se_3 sample reported as rhombohedral is slightly controversial. The second one is the reproducibility of results reported by Bera *et al.* After the Bera *et al* work, another research group (Efthimiopoulos *et al*) carried out high-pressure experiments up to ∼65 GPa on the Sb_2Se_3 compound [35]. From these systematic studies [using various pressure transmitting mediums (PTMs)], it is suggested that the influence of liquid PTM like methanol ethanol (M:E) in 4:1 ratio would cause the problem of changing the nature of the sample. They have also shown that an inert gas medium like helium can be the best PTM for this compound's high-pressure study [35]. Not only the reported TI transition but even the structural transition proposed by Bera *et al* from their Raman experiments in connection with the relevant systems were not observed by Efthimiopoulos *et al* [35]. Furthermore the Raman modes measured by Bera *et al* [39] do not match neither in frequency nor in pressure coefficient with those theoretically predicted [37]. Therefore, it can be concluded that the ongoing debate of the pressure-induced TQPT in β-Sb_2Se_3 is still open and a detailed structural characterization at ambient conditions is very essential. Recently first principle calculations reveal that the $R\bar{3}m$ structure is energetically, mechanically, and dynamically favorable at ambient conditions for Sb_2Se_3, despite the *Pnma* phase being only observed in most experiments [37]. Interestingly, both phases (*Pnma* and $R\bar{3}m$) are very competitive at ambient conditions, and the enthalpy difference between the two phases is ∼22.71 meV per formula unit at 0 K [37]. This value is lower than the room temperature thermal energy (25 meV at 300 K). Hence, it seems that the $R\bar{3}m$ phase is experimentally possible to be synthesized in Sb_2Se_3, as it has been synthesized in As_2Te_3 and As_2Se_3 [63, 64]. Since the rhombohedral phase is expected to show novel topological properties under high-pressure conditions, the first prospect would be to crystallize the Sb_2Se_3 in the $R\bar{3}m$ phase in various available synthesis routes (like high-pressure high-temperature synthesis) and study them systematically.

5.2. ABX_2 compounds

The study of pressure-induced TQPTs in ternary ABX_2 compounds has been mainly carried out in thallium- and bismuth-based chalcogenides $TlBiX_2$ (X = S, Se, Te) since this family adopts the rhombohedral (SG: $R\bar{3}m$) structure at ambient conditions; i.e. they are structurally similar to tetradymite semiconductors [65]. The rhombohedral unit cell has four atoms in which Tl, Bi, X atoms are placed in a layered fashion normal to the threefold axis in the order of –Tl–X–Bi–X– (see figure 5(a)). Here, each Tl (or Bi) layer is sandwiched between the two chalcogens (X) layers, and Tl or Bi act as the inversion centers. Therefore, there is a strong interlayer coupling that exists between them and hence makes the crystal structure 3D. Notably, this behavior is different from the tetradymite semiconductors, because there is a weak coupling (vdW type) exists between each of the quintuple layers in tetradymite semiconductors.

At ambient conditions, $TlBiS_2$ is a direct band gap semiconductor with a band gap of 0.42 eV at the Γ point. First-principles calculations predicted that $TlBiS_2$ undergoes a TQPT into a TI phase under uniaxial [along (111) direction] strain, hydrostatic pressure, and electric field [17, 20]. Moreover, a TCI phase is also predicted in $TlBiS_2$ at higher hydrostatic pressure regions (see figure 5(c)) [20]. The recent high-pressure experimental study on $TlBiS_2$ discovered the non-trivial topological phases in it [40]. The Raman linewidth anomalies of E_g mode at the pressures of ∼0.5 and ∼1.8 GPa evidence the unusual electron–phonon coupling in the rhombohedral phase of $TlBiS_2$ (see figure 6(a)) [40]. This phonon signature is linked to multiple BIs present in the systems, interpreted with the help of first-principles calculations. The first BI at Γ point (see figures 5(b) and 6(b)) changes the topological invariant quantity $\mathbb{Z}_2$ from 0 to 1 at ∼0.5 GPa (experimental transition pressure values) and therefore induces a strong TI phase in $TlBiS_2$ [40]. Further, at high-pressures (∼1.8 GPa), second BI at F point (see figures 5(c) and 6(b)) changes the mirror Chern number ($n_M = 2$), and hence induces a TCI state [40]. Upon applying further pressure, the $TlBiS_2$ undergoes a first-order structural phase transition above ∼4.0 GPa. So, in this system, the externally applied hydrostatic pressure systematically switches the direct band gap semiconductor $TlBiS_2$ to TI at ∼0.5 GPa and then into TCI at ∼1.8 GPa [40].

$TlBiS_2$ also shows a TQPT under chemical substitution. To be precise, the chemical substitution of Se at S site,

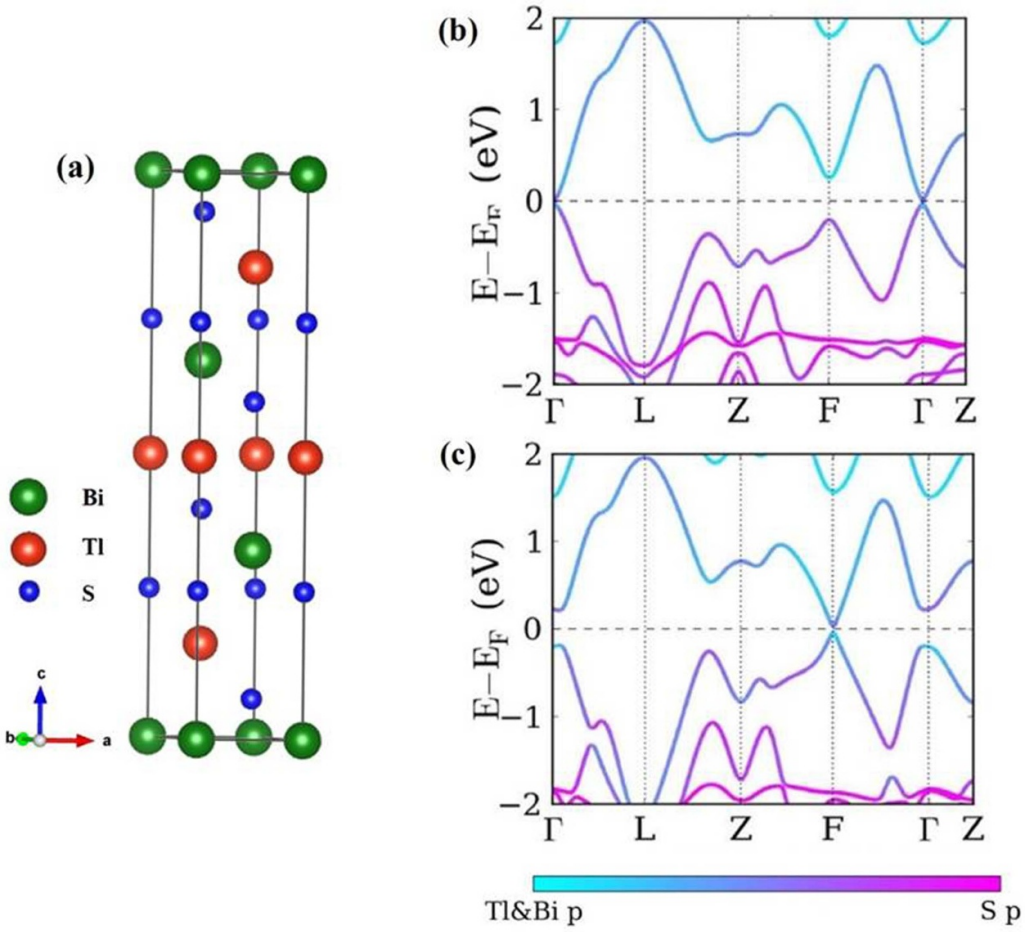

Figure 5. (a) Crystal structure of the rhombohedral phase of the $TlBiS_2$ compound. (b) The calculated electronic band structure (including the SOC effects) of the $TlBiS_2$ at 0 GPa and (c) 5.0 GPa. The first BI occurs at the Γ point of the BZ leading to the TI phase. The second BI occurs at the F point of the BZ leading to the TCI phase. The color code represents the contribution of orbital characters of Tl, Bi, and S atoms. This figure is adopted from [20].

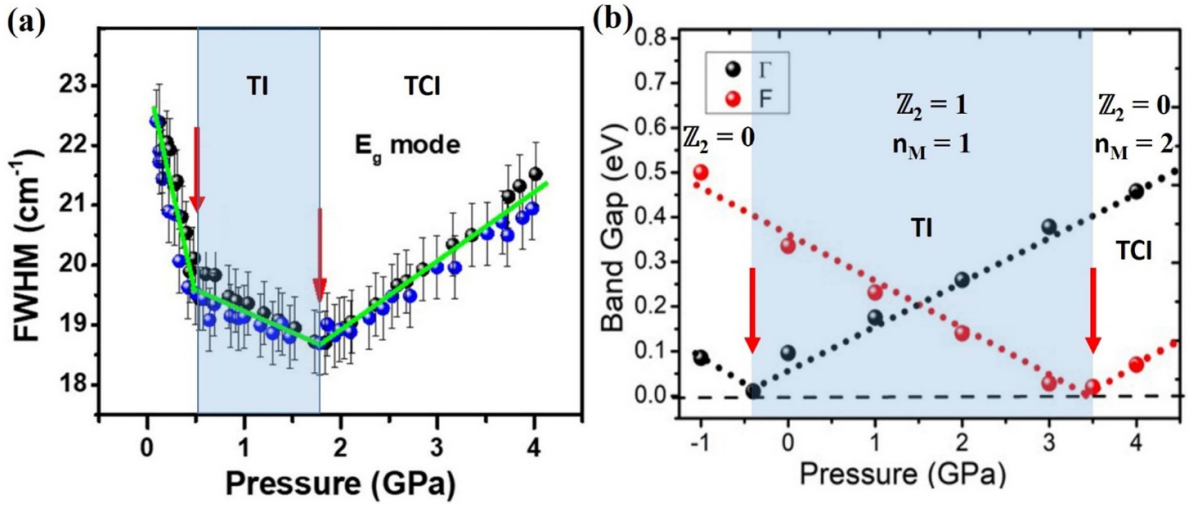

Figure 6. (a) Pressure dependence of FWHM of E_g mode in the rhombohedral phase of $TlBiS_2$. The solid red arrow at ∼0.5 GPa and ∼1.8 GPa signature the TI and TCI phases, respectively. (b) Pressure vs. band gap at the Γ and F points of the BZ. The solid red arrow at ∼−0.4 GPa and ∼3.6 GPa indicates the BI at Γ and F points of the BZ, respectively. The blue shaded region represents the TI phase. This figure is adopted from [40].

Table 1. Comparison of tetradymite and Tl-based ternary chalcogenide systems on the aspect of ambient and pressure-induced TI and TCI phases.

Compound	E_g (eV)	Space group	Theoretical prediction	Experimental Proof	TI	TCI
			Tetradymite semiconductors			
Bi_2Se_3	0.3	$R\bar{3}m$	Yes [4]	Yes [5]	Ambient	—
Bi_2Te_3	0.12	$R\bar{3}m$	Yes [4]	Yes [6]	Ambient	—
Sb_2Te_3	0.28	$R\bar{3}m$	Yes [4]	Yes [7]	Ambient	—
Sb_2Se_3	0.31[a]	$R\bar{3}m$[b]	Yes [19, 27, 33]	Yes[c]	2.5 GPa [39]	—
As_2Te_3	0.30[d]	$R\bar{3}m$	Yes [29, 30][d]	No	>2 GPa [29]	
			Tl based ternary chalcogenides			
$TlBiSe_2$	0.28	$R\bar{3}m$	—	Yes [66]	Ambient	2.5 GPa [67]
$TlBiTe_2$	0.11	$R\bar{3}m$	—	Yes [66]	Ambient	—[d]
$TlBiS_2$	0.42	$R\bar{3}m$	Yes [20]	Yes [40]	0.5 GPa [40]	1.8 GPa [40]

[a] Estimated from theoretical calculations [19].
[b] Hypothetical structure from theoretical calculations and yet to be confirmed by the XRD experiment [19, 27, 33].
[c] Yet to be reproduced by other research groups [39].
[d] Yet to be experimentally explored.

i.e. $TlBi(S_{1-x}Se_x)_2$ system, leads to the formation (at $x = 0.5$ of Se) of a single Dirac cone at the Γ point, thus showing that $TlBiSe_2$ is a TI at ambient conditions [15]. In this chemical strategy, the SOC strength of $TlBi(S_{1-x}Se_x)_2$ increases with the concentration of Se. This makes the band gap to decrease with increasing Se content, thus favoring the BI. These two combined experiments (Rajaji *et al* [40] and Sato *et al* [15]) clearly illustrate that the substitution of Se is analogous to the externally applied pressure. Pressure helps to decrease the band gap, thus acting as if the material had a stronger SOC. Further, the systematic high-pressure investigations on the tetradymite semiconductors and thallium-based III-V-VI_2 ternary chalcogenides clearly explain the following observation. When the narrow band gap compound of the 3D TI family shares the same crystal symmetry and electronic structure, but has a higher band gap (probably higher than room temperature energy ∼25 meV) and lower SOC strength, then pressure can act as a potential tool to induce the BI in the system. The obvious examples are the narrow band gap semiconductors β-As_2Te_3 ($E_g \sim 0.30$ eV), β-Sb_2Se_3 ($E_g \sim 0.31$ eV) and $TlBiS_2$ ($E_g \sim 0.42$ eV). Table 1 illustrates the relationship of the pressure-induced TQPTs to TI and TCI phases in tetradymite semiconductors and $TlBiX_2$ family.

The observation of TCI phase in $TlBiS_2$ under high pressure stimulates the keen interest in structurally similar compounds like $TlBiSe_2$ and $TlBiTe_2$. Due to a stronger SOC strength and the corresponding lower band gap (lesser than the room temperature energy), $TlBiSe_2$ and $TlBiTe_2$ are 3D TIs (show single Dirac cone at Γ point of the BZ) at ambient conditions [66]. So, if we further apply pressure to these compounds, then it might have the possibility to show the TCI phase, as $TlBiS_2$ at high pressure. Based on this intuitive idea, recently we have carried out systematic high-pressure investigations on 3D TI $TlBiSe_2$ [67]. Interestingly, it shows the TCI phase under pressure. In particular, the Raman linewidth of A_{1g} and E_g modes show the anomalies at ∼2.5 GPa, which evidence the unusual electron–phonon coupling and indicate the possible occurrence of a BI [67]. First-principles calculations confirm that it is due to a BI at the F point of the BZ and the changes in the mirror Chern number ($n_M = 2$) leading to the TCI phase [67].

The high-pressure study on Tl-based ternary chalcogenides shows multiple topological transitions [40, 67], and therefore $TlBiX_2$ family serves as the potential host for studying the topological transitions under high pressure. Moreover, the transition pressure of these systems is ⩽2.5 GPa, which can also be achieved by the chemical route. So, with the proper chemical strategy, the TCI phase can be observed in $TlBiS_2$ and $TlBiSe_2$ systems at room temperature condition. Therefore, this class of materials opens the exciting possibility to switch the TI into TCI by pressure. Further, the calculated electronic band structure of $TlBiS_2$ and $TlBiSe_2$ at high pressure shows only BIs at the Γ and F points of the BZ and almost no band overlap along other directions [20, 40, 67]. This makes the $TlBiX_2$ family to have a unique band structure and therefore are ideal candidates to study the physics behind topology, and its effect on multiple properties. Recall that the TCI phase increases the thermoelectric performance in $Pb_{0.99}Cr_{0.01}Se$ under high-pressure [31]. Similar enhancement of thermoelectric performance is expected in the $TlBiX_2$ family under high-pressure conditions during the formation of a TCI state. Therefore, it is a must to study the thermoelectric aspects for these classes of compounds.

The future perspective in this family is to study the high-pressure behavior of the $TlBiTe_2$ compound. Based on the crystal and electronic structure similarities, $TlBiTe_2$ is the potential candidate to show the TCI phase at moderate pressures. Further, the substitution of Te at the S site [i.e. $TlBi(S_{1-x}Te_x)_2$] can also possibly lead to TI property at room temperature conditions and is yet to be explored. Also, it will be interesting to make the phase diagram of $TlBiX_2$ between the pressure and the various non-trivial topological phases. In this context, transport measurements, like Shubnikov de Haas oscillation (SdH) measurements [68], are very important to be performed on the $TlBiX_2$ family. Those measurements will give insight about the Fermi surface in relation to the observed TI and TCI phases.

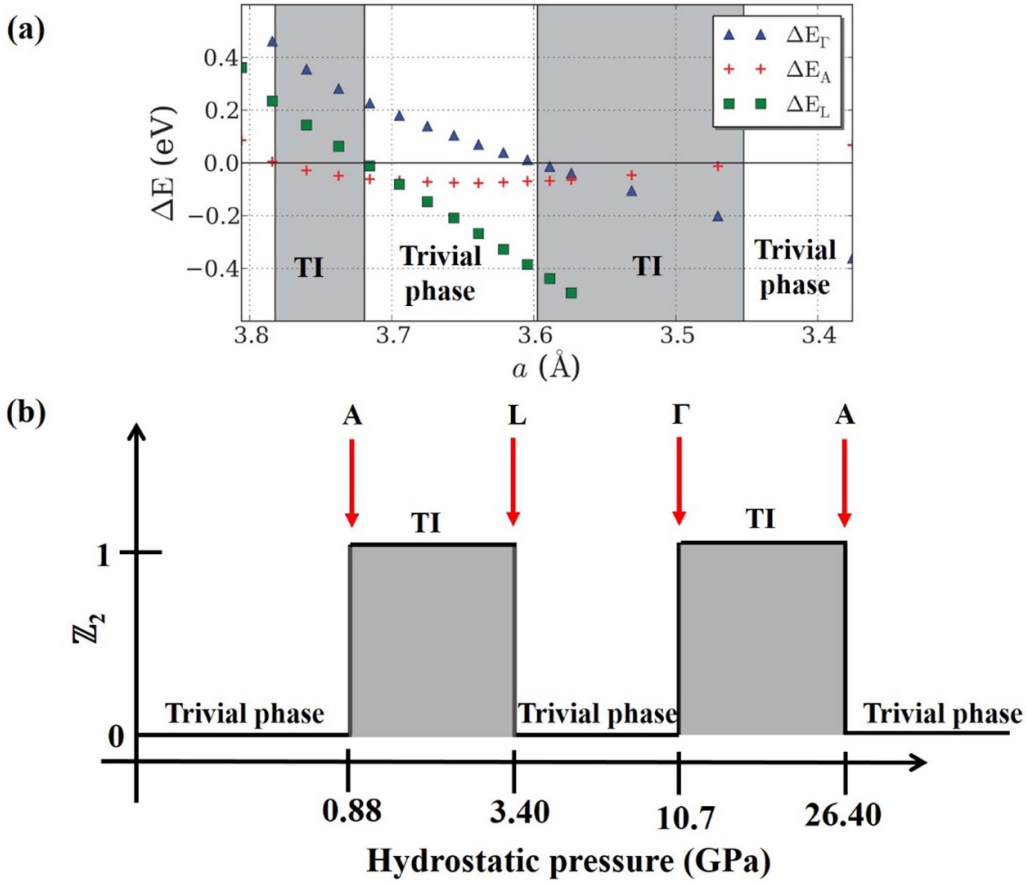

Figure 7. (a) Topological phase diagram of 1T-$TiTe_2$ under lattice compression. Here ΔE and a represent the energy difference between the states and lattice parameter, respectively. Whenever ΔE is going from a positive to a negative value, it signifies a BI. So, there is a total of four BIs indicated at A, L, Γ, and A points of the BZ. This figure is adopted from [38]. (b). Schematic representation of the oscillations of topological invariant quantity $\mathbb{Z}_2$ vs. pressure for 1T-$TiTe_2$. The solid red arrow indicates the BIs associated with the respective BZ points. The pressure values are mentioned in this figure from [53].

Before concluding this section, we will discuss some of the systems in comparison with the Tl-based ternary chalcogenide family, which might be helpful in getting a deeper understanding of TQPTs. For instance, the high-pressure phase of β-$AgBiSe_2$ (SG: $R\bar{3}m$) shares a similar crystal structure and chemistry with the 3D TI $TlBiSe_2$, but β-$AgBiSe_2$ does not show a TQPT at high pressure [44]. This example might demonstrate that just having structurally similar systems and strong SOC strength need not be a sufficient condition for achieving a TQPT. In these two systems, one notable difference exists in terms of the lone electron pairs (LEPs). Tl^{1+} has a stereoactive LEP, whereas Ag^{1+} does not have a stereoactive LEP. Therefore, it will be interesting to investigate the role played by the LEPs in the pressure-induced TQPTs of these systems and other pressure-induced TIs, which might give a more fundamental understanding of TIs in connection with the LEP chemistry.

5.3. AX_2 compounds

The study of pressure-induced TQPTs in binary AX_2 compounds has been mainly carried out in titanium-based transition metal dichalcogenides (TMDs) TiX_2. Strain (uniaxial, biaxial, and hydrostatic) induced several TQPTs have been predicted in the 1T phase (SG: $P\bar{3}m1$) of TMD $TiTe_2$ [38]. Interestingly, 1T-$TiTe_2$ compound showed (theoretical calculation) that series of topologically trivial → non-trivial → trivial → non-trivial → trivial phases under hydrostatic pressure up to ∼30 GPa (see figures 7(a) and (b)) [38]. Strongly motivated by this prediction, our group has experimentally explored the signatures of some of the predicted TQPTs [53]. The phonon anomalies of A_{1g} and E_g modes at ∼2.0 GPa and ∼4.0 GPa evidence the unusual electron–phonon coupling in 1T-$TiTe_2$ as shown in figure 8(a) [53]. In addition to that, the axial *c/a* ratio shows signatures of charge density redistributions, and electrical transport measurements revealed anomalies around similar pressures [53]. Therefore, the isostructural electronic transitions at ∼2.0 GPa and 4.0 GPa indicate the occurrence of BIs at A and L points of the BZ, respectively. The experiments confirm that the pressure-induced topologically non-trivial phase ($\mathbb{Z}_2 = 1$) and trivial metallic phase ($\mathbb{Z}_2 = 0$) at ∼2.0 GPa and ∼4.0 GPa respectively [53]. But after ∼8.0 GPa, 1T-$TiTe_2$ undergoes a structural transition from trigonal to monoclinic (SG: C2/m) phase [53]. This structural transition masks the observation of two more BIs (at Γ and A points) predicted (see figures 7(a) and (b)) in 1T-$TiTe_2$

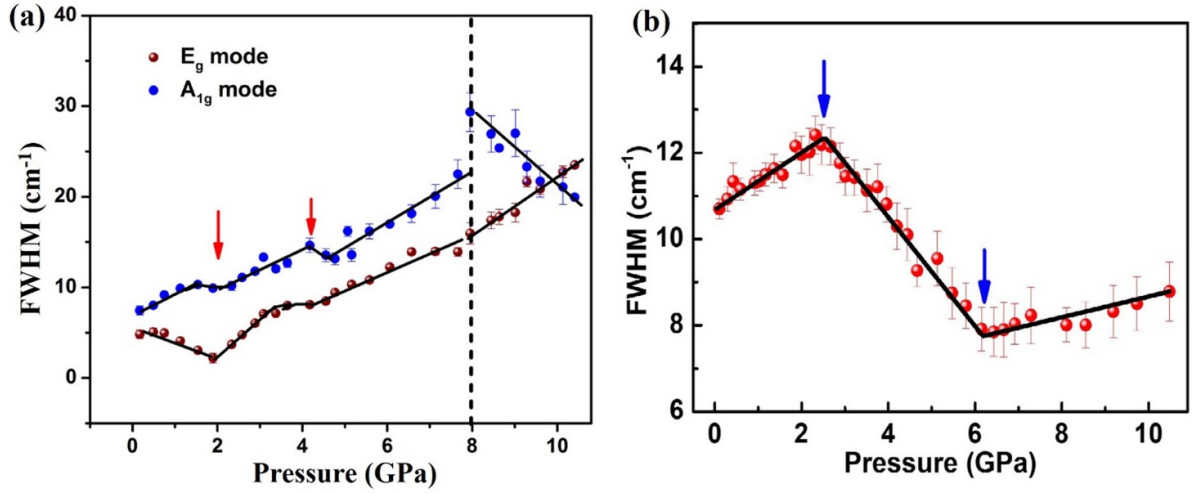

Figure 8. (a) Pressure dependence of FWHM of A_{1g} and E_g modes in 1T-$TiTe_2$. The vertical dotted lines at ∼8.0 GPa represent the first-order structural phase transition. The solid red arrows at ∼2.0 GPa and ∼4.0 GPa indicate the TI and trivial phases, respectively. (b) Pressure vs. FWHM of A_{1g} phonon mode for the 1T-$TiSe_2$ compound. The solid blue arrows at ∼2.0 GPa and ∼6.0 GPa indicate the isostructural electronic transitions associated with the TI and trivial phase, respectively. This figure is adopted from [53] and [54].

at higher pressure regions (around 10.7 GPa and 26.40 GPa). It must be stressed that these high-pressure results on the 1T-$TiTe_2$ compound were reproduced by Zhang *et al* [69]. Structural prototype 1T-$TiSe_2$ also showed similar pressure evolution of oscillation of topologically trivial → non-trivial → trivial phases from first-principles theoretical calculations [70]. The recent high-pressure experiments have confirmed this prediction using Raman signatures of A_{1g} phonon mode, as shown in figure 8(b) [54].

Even though both systems (1T-$TiTe_2$ and 1T-$TiSe_2$) share a similar crystal symmetry, the number of BIs and their associated TRIM points are different upon the application of hydrostatic pressure. There are a total of four BIs (A, L, Γ, and A) predicted for 1T-$TiTe_2$ [38], whereas two consecutive BIs (at the same Γ point) are predicted for 1T-$TiSe_2$ [70]. Hence it will be an interesting perspective to study the $TiTe_{2-x}Se_x$ compounds (both experiments and theoretical band structure calculations) because these compounds would create chemical pressure, which might be equivalent to external hydrostatic pressure. Therefore, it can have the possibility to induce some TQPTs at ambient conditions in some selective composition. Also, these two studies only showed the topological invariant quantity $\mathbb{Z}_2$ variation as a function of hydrostatic pressure. Since these two systems showed an even number of BIs, it has a possibility of forming the TCI phase under pressure. Hence it is an important prospect to study these systems under pressure as a function of mirror Chern number n_M. Moreover, 1T-$TiSe_2$ shows superconductivity in low-temperature regions and is predicted as a topological superconductor [70]. Thus it will be interesting to look for the detailed pressure-dependent transport measurements at low-temperature conditions. Finally, it is worth mentioning that 1T-TiS_2; the weak SOC compound in this family, is a semiconductor (E_g: 0.2–0.3 eV) and shares a similar crystal structure and chemistry as 1T-$TiTe_2$ and 1T-$TiSe_2$ compounds. Therefore, 1T-TiS_2 could be a potential candidate to search TQPTs at high pressures. The band structure calculations of bulk $TiS_{2-x}Te_x$ systems evidence the strong TI ($\mathbb{Z}_2 = 1$) for $x > 0.44$, which further substantiates our intuition about the pressure-induced TI phase in TiS_2 compound [71].

5.4. ABX compounds

The study of pressure-induced TQPTs in ternary ABX compounds has been mainly carried out in bismuth tellurohalides BiTeX (X = Br, I). They are strong SOC compounds with a non-centrosymmetric trigonal crystal structure (SG: $P3m1$) at ambient conditions and a giant bulk-Rashba spin splitting [24, 57, 68]. In this family, BiTeI is a polar semiconductor ($E_g \sim 0.38$ eV) at ambient conditions, and structurally, it is composed of triple layers (Te–Bi–I) stacked along the c axis through weak vdW interactions. Hydrostatic pressure-induced TI state was predicted in this non-centrosymmetric system at around 1.7–4.1 GPa [18]. The unusual decrease of Raman line width of the E mode signatures the TQPT transition in BiTeI at around 3 GPa [55]. In addition to that, the charge density fluctuations are noticed during the BI occurrence in the system through the minimum in c/a ratio at around 2.0–2.9 GPa in synchrotron XRD measurements [24]. Further, IR spectroscopy measurements (reflectance and transmittance) confirm the reduction of light absorption during the TQPT around similar pressures. Specifically, the carrier spectral weight (directly proportional to Fermi velocity) and dc optical conductivity evidence the systematic increase, reaching the maximum value at ∼2.20 GPa, and then a decreasing trend is noticed under pressure as shown in the insets of figure 9 [24]. The maximum value of carrier spectral weight (see the bottom inset of figure 9) is the indication for the linear band dispersion behaviors, which is expected during the TQPT (see figure 1). So the observed trend of the carrier spectral weight illustrates the

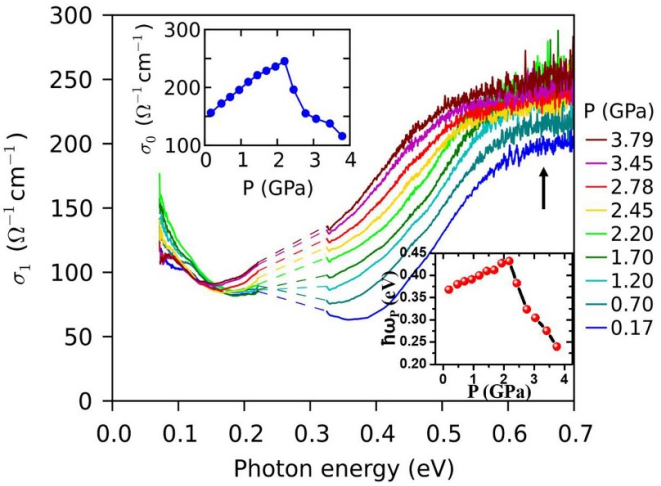

Figure 9. Pressure dependence of the real part of the optical conductivity obtained from IR spectroscopy (reflectance and transmittance) measurements in BiTeI. The solid black arrow represents the increasing pressure. The top inset shows the pressure dependence of the optical conductivity at zero photon energy (σ_0) calculated from IR spectroscopy experiments. The bottom inset shows the pressure dependence of the ω_p in the BiTeI compound. Here ${\omega_p}^2/8$ is the carrier spectral weight (is directly proportional to ${v_F}^2$) that measures the Fermi surface in weakly interacting systems. This figure is adopted from [24].

systematic band gap closing and reopening behaviors and thus confirms the signatures of the TQPT in BiTeI [24]. Importantly SdH oscillation measurements revealed that the shape of the Fermi surface changes (the inner Fermi surface increases and the outer Fermi surface decreases) significantly due to the occurrence of BIs at A point of the BZ during the TQPT in BiTeI [68].

Structural prototype BiTeBr also showed the pressure-induced TQPT at 2.9 GPa in the A point of the BZ [57]. This was confirmed by synchrotron XRD and electrical transport measurements and corroborated by the Wilson loop analysis (efficient method for non-centrosymmetric crystal structure) of the electronic states which evaluate the topologically distinct properties below and above the critical pressure [57]. It will be an exciting prospect to perform the SdH oscillation measurements on BiTeBr to get more insight into the pressure-induced TQPT on the aspect of the Fermi surface and also make the comparative analysis with the BiTeI compound. Another interesting prospect is to conduct high-pressure optical spectroscopy (both Raman and IR) experiments on the BiTeBr compound, which will give insight into the phonon linewidth anomalies, optical conductivity, and carrier spectral weight during the TQPT. Unfortunately, previous Raman measurements at high pressure in BiTeBr did not have enough quality to perform such an analysis [72].

5.5. AX compounds

The detailed experimental study of pressure-induced TQPTs in binary AX compounds has been mainly carried out in group IV–VI chalcogenides with rocksalt structure, despite TQPTs have been also predicted in other binary compounds. First principle theoretical calculations predicted several types of strain-induced TQPTs in β-InSe (SG: $P6_3/mmc$) [73], InSb [74], β-InTe (SG: $P6_3/mmc$) [75], group IV–VI semiconducting chalcogenides AX (A = Ge, Sn, Pb, and X = S, Se, Te) with a rock salt structure [76, 77], monolayer TlSe and TlS [78], etc. However, only a few experimental attempts were made in this class of compounds to explore pressure-induced TQPTs. For example, PbSe shows a TCI phase both either under high pressure or under alloying conditions. In this last case, the composition of $Pb_{1-x}Sn_xSe$ gives the formation of a TCI state $x = 0.23$ [14]. Further, the dense lead chalcogenide $Pb_{0.99}Cr_{0.01}Se$ showed the pressure-induced TCI phase transition at ∼2.8 GPa and the Raman line width of both LO and TO modes evidence the anomalies around the similar pressure regions as shown in figures 10(a) and (b) [31]. Similar to PbSe, PbTe experimentally shows a TCI phase during alloying ($Pb_{0.6}Sn_{0.4}Te$) [13] and is also predicted to exhibit a pressure-induced TQPT to a TCI phase [76]. Therefore, it will be of significance to explore the signatures of the TCI phase in PbTe at high pressure.

Mixed valent binary chalcogenide InTe (i.e. $In^{1+}In^{3+}Te^{2-}$) is an another interesting semiconductor ($E_g \sim 0.03$ eV), which adopts the tetragonal crystal structure (SG: $I\,4/mcm$) at ambient conditions [79]. The two pressure-induced BIs are predicted by theoretical calculations for InTe at Z and M points of the BZ around ∼1.0 and ∼1.4 GPa, respectively [79]. However, in this system, overall parity remains the same before and after the BI, and therefore no net changes in the topological invariant quantity $\mathbb{Z}_2$ ($\mathbb{Z}_2 = 0$ for below and above P_c) is observed [79]. Since an even number of BIs is an indication for the TCI phase, it will be an exciting prospect to perform the mirror Chern number n_M calculations and to understand the TCI phase possibility in this system. Further, it will be interesting to screen the suitable chemical dopant to change one of the parities at M and Z point of the BZ associated with their VBM and CBM during the BI in InTe. This strategy will likely induce a non-trivial topological phase in InTe compound. Finally, many of the predicted compounds are unexplored in this class, and therefore it will be exciting to perform the experimental measurements on these simple systems.

5.6. Other compounds

In addition to the above discussed families of compounds, there are several families of compounds predicted as pressure-induced TIs. For instance, monopnictide LaSb [80], ternary half-Heusler compounds [81–83], ternary chalcopyrites of composition I–III–VI_2 and II–IV–V_2 [84], Zintl compounds [85], cubic pyrochlore iridates [86], cesium-based halide perovskites [87, 88], $MnBi_2Te_4$-like materials of $MnSb_2Te_4$, $MnBi_2Se_4$, and $MnSb_2Se_4$ [89], cubic binary rare earth monopnictides family AX compounds (A = Sc, Y; X = Sb, Bi) [90], cubic bialkali antimonide KNa_2Sb [91], etc. Among these, LaSb is an interesting material that shows extreme magnetoresistance (MR) with unusual resistivity plateau [92] and also exhibits topological transition under strain. The semi-metallic compound LaSb crystallizes in a cubic structure

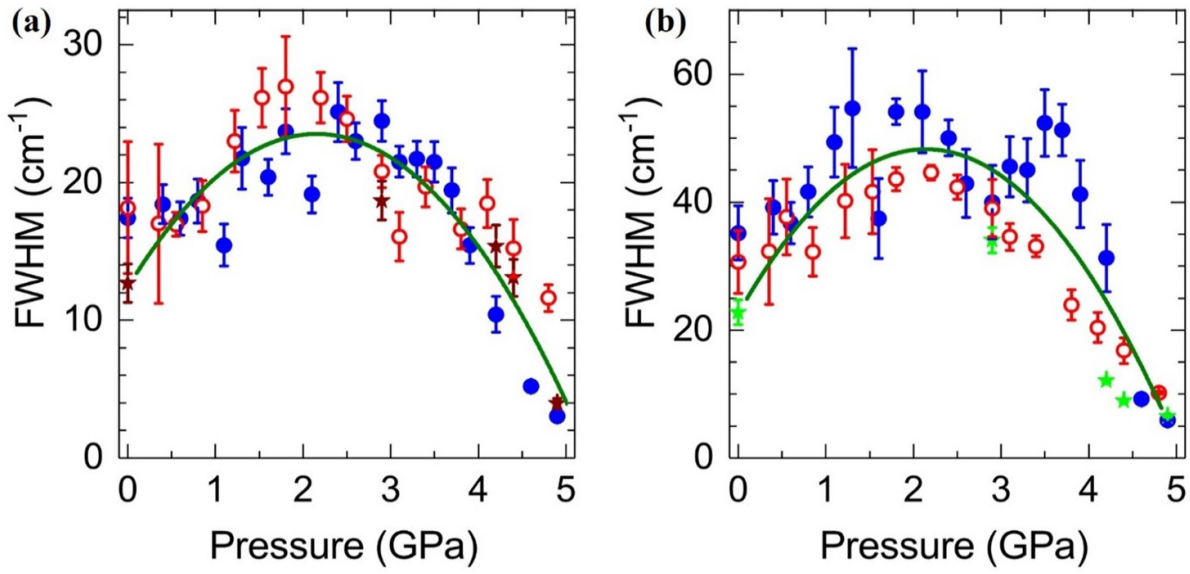

Figure 10. (a) Pressure dependence of FWHM of TO and (b). LO modes in the $Pb_{0.99}Cr_{0.01}Se$ compound for the B1 phase (SG: $Fm\bar{3}m$). Each figure represents the three sets of different experimental runs. The phonon linewidth anomalies of TO and LO phonon modes are at around ∼3.0 GPa signatures the TCI phase. This figure is adopted from [31].

of NaCl type (B1 phase, SG: $Fm\bar{3}m$) and adopts topologically trivial properties at ambient conditions [92]. First-principles electronic structure calculations predicted a pressure-induced TQPT between 3 and 4 GPa for the B1 phase [80]. Further, recent systematic high-pressure transport measurements on LaSb reveal the emergence of superconductivity [93] at ∼10.8 GPa, which originates from the structural phase transition [from cubic to tetragonal (SG: *P4/mmm*)]. Interestingly, changes in the pressure coefficient of both residual resistance and MR are observed in the B1 phase at ∼5.5 GPa and hence attributed to a possible TQPT [93]. It will be interesting to shed the light on this pressure-induced TQPT with optical spectroscopy techniques, such as Raman and IR spectroscopy (reflectance and transmittance). It is important to remember that there is no first-order Raman active mode for the cubic NaCl-type structure; however, recent systematic Raman scattering experiments in the cubic structure of the strong SOC compound $Pb_{0.99}Cr_{0.01}Se$ exhibited signatures of TO and LO phonon mode that helped to identify the pressure-induced TQPT at ∼3.0 GPa [31]. So it will be interesting to perform Raman experiments on LaSb at high pressure to get an insight into the proposed TQPT, as observed in the MR and residual resistance anomalies.

Another family that is worth to be explored is that of ternary AB_2X_4 compounds (A = Ge, Sn, Pb; B = As, Sb, Bi; X = S, Se, Te). This family result from the mixture of already mentioned AX and B_2X_3 compounds. A number of members of this family crystallize in a tetradymite-related structure (SG: $R\bar{3}m$) with septuple layers of X–B–X–A–X–B–X type instead of the quintuple layers of X–B–X–B–X type of B_2X_3 compounds [94]. Many of these Te-based compounds are predicted to be TIs at ambient conditions [94–96], and a few have been studied at high-pressure conditions [97–100]. Due to electronegativity differences, S and Se-based compounds will have a higher band gap compared to Te-based compounds. Therefore, it is expected that S- and Se-based AB_2X_4 compounds with tetradymite-like structures could lead to the observation of some pressure-induced TQPTs.

Extensive investigations (theoretical calculations) of the band structure and topological order for Pd, Pt, Au, and Ni based ternary half-Heusler compounds have been reported in the literature [81–83]. The rare-earth-based half-Heusler compound *R*PdBi [*R* (rare earth) = Y, Sm, Gd, Tb, Dy, Ho, Er, Tm, and Lu] crystallizes in the cubic non-centrosymmetric MgAgAs-type structure (SG: $F\bar{4}3m$) [81]. Here, the calculated BI strength, $\Delta E = E_{\Gamma 8} - E_{\Gamma 6}$, conventionally classifies trivial and topological materials with the criterion of $\Delta E < 0$ and $\Delta E > 0$, respectively, as shown in figure 11 [81]. In this family, the size of the rare-earth element tunes the lattice parameter, atomic number, and SOC strength. Therefore, the rare-earth size acts as analogous to external pressure. Consequently, the compounds with lighter *R* elements (Sm, Gd Tb, Dy, and Y) show a BI strength $\Delta E < 0$ and are trivial materials at ambient conditions, whereas the compounds with heavier *R* elements (Ho, Er, Tm, and Lu) show a BI strength $\Delta E > 0$ and are TIs at ambient conditions [81]. Interestingly, these systems with lighter *R* elements can be transformed into TI under external pressure, which decreases the lattice parameter. Along with TI properties, these compounds also exhibit magnetism and superconductivity. Hence they can be potential candidates for the realization of multifunctional topological devices. Another added advantage for ternary half-Heusler compounds is alloying. For instance, the alloying of the Bi (Pd) site with Sb (Ni) could also lead to the possibility of nontrivial topological phases at high pressures [82, 83]. Therefore, it would be an exciting prospect to experimentally study the *R*PdBi compounds with lighter *R* elements (Sm, Gd, Tb, Dy, and Y) under high-pressure conditions. Apart from this specific class, many Pt, Au, and Ni-based ternary thermoelectric Half-Heusler compounds are predicted as potential

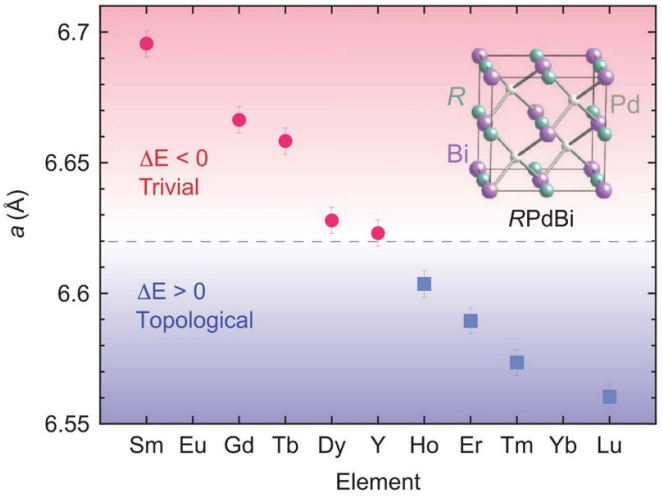

Figure 11. The plot of lattice parameter vs. lanthanides in half Heusler RPdBi compounds. Here, the dashed lines represent the critical value of the lattice parameter $a_c = 6.62$ Å. Below a_c ($\Delta E > 0$), materials are TIs whereas above a_c ($\Delta E < 0$), materials are NIs. The inset shows the cubic crystal structure of typical RPdBi compounds. This figure is adopted from [81].

pressure-induced Tis [83]. Hence many experimental studies are needed in this class of compounds that can unveil the mystery of TI's properties and are expected to have an impact on green energy technology.

Another interesting family that need to be explored for possible TQPTs is that of A_2X compounds (A = Ag; X = S, Se, Te) with exceptional MR properties. The monoclinic structure of β-Ag_2Se and β-Ag_2Te are TIs [101], and that of Ag_2S is a NI at ambient conditions. High-pressure studies of these materials have been conducted [102–105], but the pressure-induced topological transition has not been found yet. In this family it is possible that $Ag_2Se_{1-x}S_x$ compounds could be interesting to be studied for a possible TQPT since the band gap of Ag_2Se has been found to increase with pressure as it occurs in TIs after the TQPT [103]. Finally, we want to comment that recent theoretical calculations have studied the concentration and pressure effects on the topological phases of $SnSi_{1-x}Ge_x$ compounds [106]. Since these alloys are dynamically stable, it is expected that these alloys can be experimentally synthesized and studied with much interest due to their compatibility with silicon technology.

6. Conclusion and outlook

In summary, we have presented a comprehensive review of the pressure-tuned topological transitions (TIs and TCIs) on several families of compounds and provided future perspectives for each of them. Topological materials (TIs and TCIs) are playing a vital role in important technological devices such as thermoelectrics, spintronics, and quantum computers. In this way, we need to discover a variety of new quantum materials and design materials with tailored properties to achieve the above mentioned technological needs. To search for the new topological materials, one of the simplest and foremost steps is to predict the pressure-induced TIs and TCIs in the suitable SOC compounds via first-principles calculations taking into account SOC, which can effectively analyze the bulk and surface electronic band structure. In the second step, some of the important details of prediction such as the predicted crystal structure, the kind of strain (uniaxial, biaxial, hydrostatic, etc) applied in the calculations, band gap, the existence of the predicted compound in real, etc should be checked by the scientist before exploring the predicted compounds. The third step is the detection of signatures of the topological transitions with suitable experimental techniques.

Fortunately, recent theory and experiments have proved that Raman scattering is a potential and simple tool to study the pressure-induced topological transitions through electron–phonon coupling changes in strong SOC materials. Conventionally, Raman scattering (non-contact probe) is commonly used as a probe to study structural and electronic transitions, 2D materials such as graphene, TMDs, etc. Now, in this list, the exotic topological transitions can also be included. In addition to Raman spectroscopy, IR spectroscopy, SdH oscillation measurements, and electrical resistivity are also potential tools to study these pressure-induced TQPTs. Finally, we hope that this review article gives the potential ideas and will initiate a lot of interdisciplinary research work in the direction of pressure-induced TIs and TCIs.

Data availability statement

All data that support the findings of this study are included within the article (and any supplementary files).

Acknowledgments

V R and C N would like to dedicate this review to Professor C N R Rao who has been a mentor and inspiration for us. V R and C N acknowledge the Department of Science and Technology (DST) and JNCASR, India, for financial support. FJM acknowledges project MALTA Consolider Team network (RED2018-102612-T), financed by MINECO/AEI/10.13039/501100003329, I+D+i project PID2019-106383GB-42 financed by MCIN/AEI/10.13039/501100011033, as well as projects PROMETEO/2018/123 (EFIMAT) and CIPROM/2021/075 (GREENMAT) financed by Generalitat Valenciana. We sincerely thank Professor Umesh V Waghmare, Theoretical Sciences Unit, JNCASR, Professor Kanishka Biswas, New Chemistry Unit, JNCASR, Professor Sebastian C Peter, New Chemistry Unit, JNCASR, and Dr Boby Joseph, Elettra Sincrotrone Trieste, Italy for the active collaboration and fruitful discussion on these topics of interest.

ORCID iDs

V Rajaji https://orcid.org/0000-0002-7913-5826
F J Manjón https://orcid.org/0000-0002-3926-1705
Chandrabhas Narayana https://orcid.org/0000-0001-6256-8994

References

[1] Hasan M Z and Kane C L 2010 *Rev. Mod. Phys.* **82** 3045
[2] Bernevig B A, Hughes T L and Zhang S-C 2006 *Science* **314** 1757
[3] König M, Wiedmann S, Brüne C, Roth A, Buhmann H, Molenkamp L W, Qi X-L and Zhang S-C 2007 *Science* **318** 766
[4] Zhang H, Liu C-X, Qi X-L, Dai X, Fang Z and Zhang S-C 2009 *Nat. Phys.* **5** 438
[5] Xia Y *et al* 2009 *Nat. Phys.* **5** 398
[6] Chen Y L *et al* 2009 *Science* **325** 178
[7] Hsieh D *et al* 2009 *Phys. Rev. Lett.* **103** 146401
[8] Fu L, Kane C L and Mele E J 2007 *Phys. Rev. Lett.* **98** 106803
[9] Majhi K, Pal K, Lohani H, Banerjee A, Mishra P, Yadav A K, Ganesan R, Sekhar B R, Waghmare U V and Anil Kumar P S 2017 *Appl. Phys. Lett.* **110** 162102
[10] Gresch D, Autès G, Yazyev O V, Troyer M, Vanderbilt D, Bernevig B A and Soluyanov A A 2017 *Phys. Rev.* B **95** 075146
[11] Jeffrey C Y, Teo L F and Kane C L 2008 *Phys. Rev.* B **78** 045426
[12] Liang F 2011 *Phys. Rev. Lett.* **106** 106802
[13] Xu S-Y *et al* 2012 *Nat. Commun.* **3** 1192
[14] Dziawa P *et al* 2012 *Nat. Mater.* **11** 1023
[15] Sato T, Kouji Segawa K, Souma K S, Nakayama K, Eto K, Minami T, Ando Y and Takahashi T 2011 *Nat. Phys.* **7** 840
[16] Hasan M Z, Xu S-Y and Neupane M 2015 *Topol. Insul.* 55
[17] Singh B, Lin H, Prasad R and Bansil A 2014 *J. Appl. Phys.* **116** 033704
[18] Bahramy M S, Yang B J, Arita R and Nagaosa N 2012 *Nat. Commun.* **3** 679
[19] Li W, Wei X-Y, Zhu J-X, Ting C S and Chen Y 2014 *Phys. Rev.* B **89** 035101
[20] Zhang Q, Cheng Y and Schwingenschlögl U 2015 *Sci. Rep.* **5** 8379
[21] Xu B, Zhao L X, Marsik P, Sheveleva E, Lyzwa F, Dai Y M, Chen G F, Qiu X G and Bernhard C 2018 *Phys. Rev. Lett.* **121** 187401
[22] Fan Z, Liang Q-F, Chen Y B, Yao S-H and Zhou J 2017 *Sci. Rep.* **7** 45667
[23] Zholudev M S *et al* 2019 *Condens. Matter* **4** 27
[24] Xi X, Ma C, Liu Z, Chen Z, Ku W, Berger H, Martin C, Tanner D B and Carr G L 2013 *Phys. Rev. Lett.* **111** 155701
[25] Rusinov I P, Menshchikova T V, Sklyadneva I Y, Heid R, Bohnen K P and Chulkov E V 2016 *New J. Phys.* **18** 113003
[26] Yamaoka H, Jeschke H O, Yang X, He T, Goto H, Hiraoka N, Ishii H, Mizuki J and Kubozono Y 2020 *Phys. Rev.* B **102** 155118
[27] Liu W, Peng X, Tang C, Sun L, Zhang K and Zhong J 2011 *Phys. Rev.* B **84** 245105
[28] Lima M P, Besse R and Da Silva J L F 2020 *J. Phys.: Condens. Matter* **33** 025003
[29] da Silva E L, Leonardo A, Yang T, Santos M C, Vilaplana R, Gallego-Parra S, Bergara A and Manjón F J 2021 *Phys. Rev.* B **104** 024103
[30] Pal K and Waghmare U V 2014 *Appl. Phys. Lett.* **105** 062105
[31] Chen L-C, Chen P-Q, Li W-J, Zhang Q, Struzhkin V V, Goncharov A F, Ren Z and Chen X-J 2019 *Nat. Mater.* **18** 1321
[32] Pal K, Anand S and Waghmare U V 2015 *J. Mater. Chem.* C **3** 12130
[33] Cao G, Liu H, Liang J, Cheng L, Fan D and Zhang Z 2018 *Phys. Rev.* B **97** 075147
[34] Hobson T D C, Hutter O S, Birkett M, Veal T D and Durose K 2018 *Presented at the 2018 IEEE 7th World Conf. on Photovoltaic Energy Conversion (WCPEC) (A Joint Conf. of 45th IEEE PVSC, 28th PVSEC & 34th EU PVSEC)* (unpublished) (https://doi.org/10.1109/PVSC.2018.8547622)
[35] Efthimiopoulos I, Zhang J, Kucway M, Park C, Ewing R C and Wang Y 2013 *Sci. Rep.* **3** 2665
[36] Matetskiy A V, Mararov V V, Kibirev I A, Zotov A V and Saranin A A 2020 *J. Phys.: Condens. Matter* **32** 165001
[37] Skelton J M, da Silva E L, Rodríguez-Hernández P, Muñoz A, Santos M C, Martínez-García D, Vilaplana R and Manjón F J 2022 (arxiv:2206.01025)
[38] Zhang Q, Cheng Y and Schwingenschlögl U 2013 *Phys. Rev.* B **88** 155317
[39] Bera A, Pal K, Muthu D V S, Sen S, Guptasarma P, Waghmare U V and Sood A K 2013 *Phys. Rev. Lett.* **110** 107401
[40] Rajaji V, Arora R, Sarma S C, Joseph B, Peter S C, Waghmare U V and Narayana C 2019 *Phys. Rev.* B **99** 184109
[41] Haubold E *et al* 2019 *APL Mater.* **7** 121106
[42] Cuenca-Gotor V P *et al* 2020 *Phys. Chem. Chem. Phys.* **22** 3352
[43] Nayak A P, Bhattacharyya S, Zhu J, Liu J, Wu X, Pandey T, Jin C, Singh A K, Akinwande D and Lin J-F 2014 *Nat. Commun.* **5** 3731
[44] Rajaji V *et al* 2016 *Appl. Phys. Lett.* **109** 171903
[45] Manjón F J *et al* 2013 *Phys. Status Solidi* b **250** 669
[46] Polian A, Gauthier M, Souza S M, Trichês D M, de Lima J C and Grandi T A 2011 *Phys. Rev.* B **83** 113106
[47] Blanter Y M, Kaganov M I, Pantsulaya A V and Varlamov A A 1994 *Phys. Rep.* **245** 159
[48] Lifshitz I M 1960 *Sov. Phys. JETP* **11** 1130
[49] Vilaplana R *et al* 2011 *Phys. Rev.* B **84** 104112
[50] Gomis O, Vilaplana R, Manjón F J, Rodríguez-Hernández P, Pérez-González E, Muñoz A, Kucek V and Drasar C 2011 *Phys. Rev.* B **84** 174305
[51] Vilaplana R *et al* 2011 *Phys. Rev.* B **84** 184110
[52] Zhao K, Lv Y-F, Ji S-H, Ma X, Xi C and Xue Q-K 2014 *J. Phys.: Condens. Matter* **26** 394003
[53] Rajaji V, Dutta U, Sreeparvathy P C, Sarma S C, Sorb Y A, Joseph B, Sahoo S, Peter S C, Kanchana V and Narayana C 2018 *Phys. Rev.* B **97** 085107
[54] Rajaji V, Janaky S, Sarma S C, Peter S C and Narayana C 2019 *J. Phys.: Condens. Matter* **31** 165401
[55] Ponosov Y S, Kuznetsova T V, Tereshchenko O E, Kokh K A and Chulkov E V 2014 *JETP Lett.* **98** 557
[56] Saha K, Légaré K and Garate I 2015 *Phys. Rev. Lett.* **115** 176405
[57] Ohmura A, Higuchi Y, Ochiai T, Kanou M, Ishikawa F, Nakano S, Nakayama A, Yamada Y and Sasagawa T 2017 *Phys. Rev.* B **95** 125203
[58] Jones R O 2022 *J. Phys.: Condens. Matter* **34** 343001
[59] Cheng Y, Cojocaru-Mirédin O, Keutgen J, Yu Y, Küpers M, Schumacher M, Golub P, Raty J-Y, Dronskowski R and Wuttig M 2019 *Adv. Mater.* **31** 1904316
[60] Golden J C, Vinh H and Lubchenko V 2017 *J. Chem. Phys.* **146** 174502
[61] Sorb Y A, Rajaji V, Malavi P S, Subbarao U, Halappa P, Peter S C, Karmakar S and Narayana C 2015 *J. Phys.: Condens. Matter* **28** 015602
[62] Efthimiopoulos I, Kemichick J, Zhou X, Khare S V, Ikuta D and Wang Y 2014 *J. Phys. Chem.* A **118** 1713
[63] Morin C *et al* 2015 *Inorg. Chem.* **54** 9936
[64] Lityagina L M, Kulikova L F, Zibrov I P, Dyuzheva T I, Nikolaev N A and Brazhkin V V 2015 *J. Alloys Compd.* **644** 799
[65] Teske C L and Bensch W 2006 *Acta Crystallogr.* E **62** i163
[66] Chen Y L *et al* 2010 *Phys. Rev. Lett.* **105** 266401

[67] Rajaji V, Arora R, Roychowdhury S, Joseph B, Wagmare U V, Biswas K and Narayana C submitted
[68] Park J, Jin K-H, Jo Y J, Choi E S, Kang W, Kampert E, Rhyee J S, Jhi S-H and Kim J S 2015 *Sci. Rep.* **5** 15973
[69] Zhang M, Wang X, Rahman A, Zeng Q, Huang D, Dai R, Wang Z and Zhang Z 2018 *Appl. Phys. Lett.* **112** 041907
[70] Zhu Z, Cheng Y and Schwingenschlögl U 2014 *Sci. Rep.* **4** 4025
[71] Zhu Z, Cheng Y and Schwingenschlögl U 2013 *Phys. Rev. Lett.* **110** 077202
[72] Sans J A *et al* 2016 *Phys. Rev.* B **93** 024110
[73] Ma Y, Dai Y, Yu L, Niu C and Huang B 2013 *New J. Phys.* **15** 073008
[74] Feng W, Zhu W, Weitering H H, Stocks G M, Yao Y and Xiao D 2012 *Phys. Rev.* B **85** 195114
[75] Irudin Hashimzade F, Huseinova D, Jahangirli Z, Mamedov N and Mehdiyev B 2017 (available at: www.researchgate.net/publication/319312117_A_new_topological_insulator_-_beta-InTe_strained_in_the_layer_plane)
[76] Barone P, Rauch T, Di Sante D, Henk J, Mertig I and Picozzi S 2013 *Phys. Rev.* B **88** 045207
[77] Aguado-Puente P, Fahy S and Grüning M 2020 *Phys. Rev. Res.* **2** 043105
[78] Niu C, Buhl P M, Bihlmayer G, Wortmann D, Blügel S and Mokrousov Y 2015 *Nano Lett.* **15** 6071
[79] Rajaji V, Pal K, Sarma S C, Joseph B, Peter S C, Waghmare U V and Narayana C 2018 *Phys. Rev.* B **97** 155158
[80] Guo P-J, Yang H-C, Liu K and Lu Z-Y 2017 *Phys. Rev.* B **96** 081112
[81] Nakajima Y *et al* 2015 *Sci. Adv.* **1** e1500242
[82] Lin H, Wray L A, Xia Y, Xu S, Jia S, Cava R J, Bansil A and Hasan M Z 2010 *Nat. Mater.* **9** 546
[83] Chadov S, Qi X, Kübler J, Fecher G H, Felser C and Zhang S C 2010 *Nat. Mater.* **9** 541
[84] Feng W, Xiao D, Ding J and Yao Y 2011 *Phys. Rev. Lett.* **106** 016402
[85] Sun Y, Chen X-Q, Franchini C, Li D, Yunoki S, Li Y and Fang Z 2011 *Phys. Rev.* B **84** 165127
[86] Yang B-J and Kim Y B 2010 *Phys. Rev.* B **82** 085111
[87] Yalameha S, Saeidi P, Nourbakhsh Z, Vaez A and Ramazani A 2020 *J. Appl. Phys.* **127** 085102
[88] Afsari M, Boochani A, Hantezadeh M and Elahi S M 2017 *Solid State Commun.* **259** 10
[89] Zhang H, Yang W, Wang Y and Xu X 2021 *Phys. Rev.* B **103** 094433
[90] Narimani M and Nourbakhsh Z 2020 *J. Phys. Chem. Solids* **145** 109537
[91] Sklyadneva I Y, Rusinov I P, Heid R, Bohnen K P, Echenique P M and Chulkov E V 2016 *Sci. Rep.* **6** 24137
[92] Zeng L K *et al* 2016 *Phys. Rev. Lett.* **117** 127204
[93] Zhang M, Wang X, Rahman A, Dai R, Wang Z and Zhang Z 2020 *Phys. Rev.* B **101** 064106
[94] Menshchikova T V, Eremeev S V and Chulkov E V 2013 *Appl. Surf. Sci.* **267** 1
[95] Niesner D *et al* 2014 *Phys. Rev.* B **89** 081404
[96] Eremeev S V, Menshchikova T V, Silkin I V, Vergniory M G, Echenique P M and Chulkov E V 2015 *Phys. Rev.* B **91** 245145
[97] Hsieh W-P, Zalden P, Wuttig M, Lindenberg A M and Mao W L 2013 *Appl. Phys. Lett.* **103** 191908
[98] Vilaplana R *et al* 2016 *J. Alloys Compd.* **685** 962
[99] Song P, Matsumoto R, Hou Z, Adachi S, Hara H, Saito Y, Castro P B, Takeya H and Takano Y 2020 *J. Phys.: Condens. Matter* **32** 235901
[100] Sans J A *et al* 2020 *Inorg. Chem.* **59** 9900
[101] Zhang W, Yu R, Feng W, Yao Y, Weng H, Dai X and Fang Z 2011 *Phys. Rev. Lett.* **106** 156808
[102] Zhao Z, Wang S, Zhang H and Mao W L 2013 *Phys. Rev.* B **88** 024120
[103] Zhao Z, Wang S, Oganov A R, Chen P, Liu Z and Mao W L 2014 *Phys. Rev.* B **89** 180102
[104] Santamaría-Pérez D, Marqués M, Chuliá-Jordán R, Menendez J M, Gomis O, Ruiz-Fuertes J, Sans J A, Errandonea D and Recio J M 2012 *Inorg. Chem.* **51** 5289
[105] Zhao Z, Wei H and Mao W L 2016 *Appl. Phys. Lett.* **108** 261902
[106] Yalameha S and Nourbakhsh Z 2022 *Mater. Sci. Eng.* B **281** 115742